Computing Shortest Homotopic Cycles on Polyhedral Surfaces with Hyperbolic Uniformization Metric

Miao Jin[a], Ning Ding[a], Yang Yang[a]

[a] *Center for Advanced Computer Studies, University of Louisiana at Lafayette*

Abstract

The problem of computing shortest homotopic cycles on a surface has various applications in computational geometry and graphics. In general, shortest homotopic cycles are not unique, and local shortening algorithms can become stuck in local minima. For surfaces with negative Euler characteristic that can be given a hyperbolic uniformization metric, however, we show that they are unique and can be found by a simple locally shortening algorithm. We also demonstrate two applications: constructing extremal quasiconformal mappings between surfaces with the same topology, which minimize angular distortion, and detecting homotopy between two paths or cycles on a surface.

Keywords: Unique Shortest Homotopic Cycle, Hyperbolic Uniformization Metric, Local Loop Shortening, Extremal Quasiconformal Mapping, Homotopy Detection

1. Introduction

Various geometric problems directly depend on or are closely related to the computation of shortest homotopic cycles for surfaces with complex topology, including loop contractibility [1, 2], homotopy detection [3], optimal cut and pants decomposition [4, 5], shortest cut graphs [6, 7], shortest generators for homotopy or homology groups [8, 9], shortest non-trivial cycles [10, 11], and shortest essential cycles [12]. Applications of these basic algorithms include topology repair of 3D models [13, 14], denoising [8], parametrization and remeshing [15], surface matching and morphing [16], and feature recognition [17, 18].

Most of the previous works [19, 20, 21, 22, 23, 24, 25, 26, 27, 4, 5, 28] consider the shortest homotopic cycle problem on either combinatorial surfaces or piecewise-linear surfaces. The best result, to our knowledge, is given

by Colin de Verdière and Erickson [28] with time complexity $O(gnk \log(nk))$, where g and n are the genus and the complexity of the combinatorial surface respectively, and k is the number of edges of the input cycle. Their computation of the shortest cycle homotopic to a given cycle of complexity k is based on the preprocessing of the surface: a tight octagonal decomposition of the surface in $O(n^2 \log n)$ time.

In general, a closed geodesic in a given homotopic type is not unique, and local shortening algorithms can become stuck in local minima, as illustrated by Figure 1. Complicated global processing algorithms are required. However, if we consider topologically non-trivial surfaces (i.e., *genus* > 1), according to the Uniformization theorem [29], there exists a hyperbolic uniformization metric such that whose Gaussian curvature is constantly negative everywhere on the surface. It is not difficult to prove that there exists a unique closed geodesic, a cycle with global minimal length, in each homotopy class for surfaces with negative Gaussian curvature. With no local minima, any simple local shortening algorithm can theoretically be adapted to find out the shortest cycle homotopic to a given cycle on a surface with non-trivial topology. For surfaces with a Riemannian metric, several algorithms locally shorten curves, including Birkhoff curve shortening [30], disk flow [31], and geodesic curvature flow [19, 20]. We adopt Birkhoff curve shortening in this paper for its simplicity.

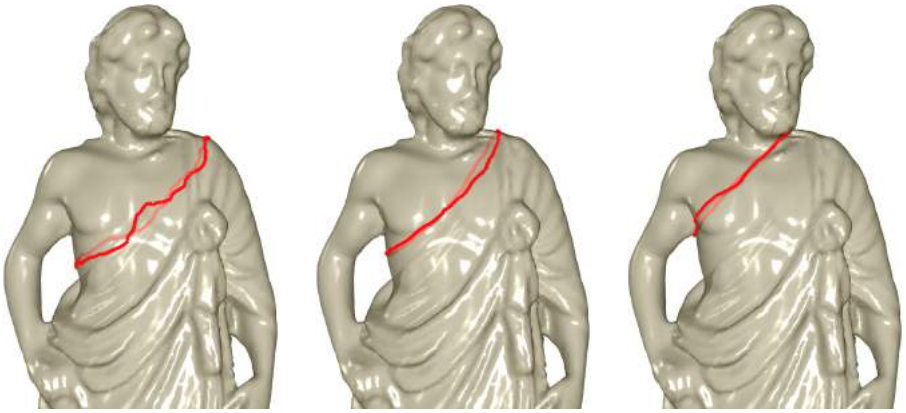

(a) (b) (c)

Figure 1: A local loop shortening process may become stuck at a local minima. (a) original loop on Greek model (b) shortening the input loop after 2 iterations. (c) shortening after 5 iterations.

The computation of the closed shortest homotopic cycle based on a surface hyperbolic uniformization metric can simplify the algorithm design, and provides different solutions of related problems. We provide two applications in this paper.

Constructing a smooth and one-to-one mapping with the least global distortion between surfaces provides a useful tool for numerous applications in computer graphics, geometric modeling, and visualization, where mapping quality is largely measured by the introduced angular distortion. It is a fundamental but challenging problem especially for surfaces with complicated topology. In general, there does not exist an angle preserved mapping between two arbitrary topologically equivalent surfaces, but among all possible diffeomorphisms between the two surfaces, the extremal quasiconformal mapping, the one minimizing the angular distortion the most, exists. Geodesic spectrum - sorted closed shortest homotopic cycles according to their lengths under the measurement of surface hyperbolic uniformization metric - guides us to approximate the extremal quasiconformal mapping between surfaces.

The other application is homotopy detection, whether two paths or cycles are homotopic to each other. We can pick the unique geodesic under surface hyperbolic uniformization metric in each homotopy class as its representative and solve the problem that whether two closed cycles are homotopic to each other by checking whether they share the same homotopy representative. For topologically trivial cycles, they will of course shrink to points.

1.1. Related Works

In this paper, we study the problem of finding the unique shortest cycle homotopic to a given cycle on a topological nontrivial polyhedral surface based on surface hyperbolic uniformization metric. Previous works have considered the related questions of finding the shortest path in a surface that is homotopic to a given path, or the shortest cycle that is either homotopic or homologous to a given cycle based on surface Riemannian metric. For computing shortest paths, We refer readers to the comprehensive survey by Mitchell [32].

Geodesic curvature flow based methods [19, 20, 21, 22, 23, 24] deform the cycle on surface to a local minimum within the same homotopy type. Hershberger and Snoeyink [25, 26] compute the shortest path or cycle homotopic to a given path or cycle of a piecewise linear surface where all the triangle vertices lie on the boundary. Yin et. al. [27] apply the shortest path

algorithm to compute the shortest cycle in each homotopy class of a polyhedral surface with general topology by constructing the Universal Covering Space. Colin de Verdière and Lazarus [4, 5] introduce algorithms to compute the shortest simple loop or cycle homotopic to a given simple loop or cycle, in time polynomial in the complexity of the surface, the complexity of the input curve, and the ratio between the largest and smallest edge lengths. A generalized algorithm is given by Colin de Verdière and Erickson [28] to compute the shortest cycle (either simple or not) homotopic to a given cycle in a combinatorial surface with genus g and complexity n in $O(gnk \log(nk))$ time, where k is the number of edges of the input cycle.

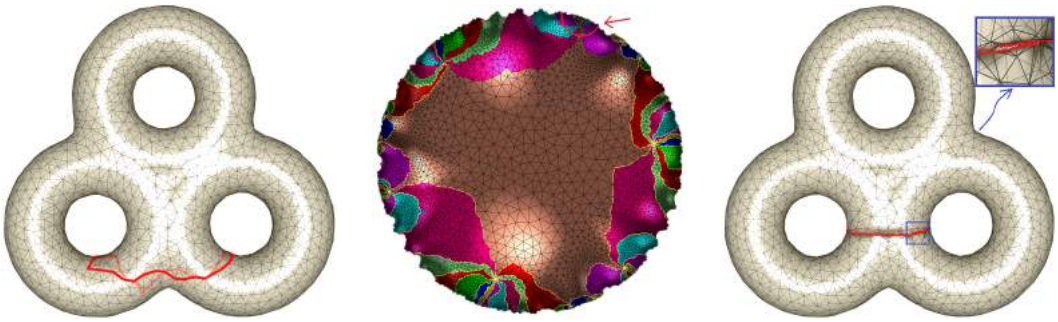

(a) (b) (c)

Figure 2: Previous universal covering space based methods for finding the closed geodesic [33, 34]: (a) the original loop on surface. (b) The red arc, as indicated by the arrow, is the axis of the Fuchsian transformation of the given homotopy type (homotopic to the original loop). The projection of the red arc from the universal covering space to the original 3-hole surface induces the loop as illustrated in (c), the closed geodesic in the given homotopy type. (c) Without the exact computation which greatly increases the computational complexity, the projection is not a closed loop due to accumulation error of the computation of universal covering space, as shown by the zoom in.

In [35], Chambers et al. prove that finding the shortest cycle (either simple or not) in a given homology class in a surface graph is NP-hard; Chen and Friedman [36, 37] prove that the corresponding problem in simplicial complexes is NP-hard to approximate within any constant factor. Dey et al. [8] propose the persistence based algorithm to compute tunnel and handle loops which are defined via homology and apply for topological denoising. Let G be a directed graph with weighted edges, embedded on a surface of genus g, b boundaries, and complexity n, Erickson and Nayyeri [38] propose

an algorithm to compute the shortest directed cycle in G in any given $\mathbb{Z}_2$ homology class in $2^{O(g+b)}n \log n$ time.

The only previous works based on surface hyperbolic uniformization metric use an algebraic way to compute the closed geodesic for a given homotopy type on surfaces with $\chi < 0$ [33, 34], by projecting the axis of the Fuchsian transformation corresponding to the homotopy type from universal covering space to the original surface. The cost of the method is not only the computation of the universal covering space and its storage, but also the extremely high requirement of computational accuracy, as illustrated in Figure 2.

The outline of the paper is as follows. In Section 2, we introduce the concepts which are necessary to the algorithms which include the theoretical foundation of this paper. In Section 3, we give a brief review of one local loop shortening algorithm. We give the details of the algorithms in Section 4. In Section 5, we give experimental results and discussions. We then further show two applications in Section 6. In Section 7, we conclude our paper and give future directions.

2. Uniformization Metric and Unique Closed Homotopy Geodesic

In this section, we give a brief review of the concepts which are necessary to this paper. The details can be found from classical textbooks in algebraic topology [39] and Riemannian geometry [40]. We also introduce the Geodesic Uniqueness theorem that states that there exists only one unique globally shortest geodesic and no any other locally shortest ones in each homotopy class for surfaces with hyperbolic uniformization metrics. The theorem is the foundation of this paper. Surface Ricci flow, a tool to compute surface hyperbolic uniformization metric, is also introduced.

2.1. Homotopy

Two closed curves γ and $\bar{\gamma}$ on a surface M are *homotopic* to each other if there is a continuous map $h : [0, 1] \times S^1 \to M$ such that $h(0, t) = \gamma(t)$ and $h(1, t) = \bar{\gamma}(t)$ for all t. A loop is contractible if it is homotopic to a constant point. In simple words, two loops are homotopic if they can deform to each other without leaving the surface. A loop is contractible if it can shrink to a point on the surface. So all the closed loops on the surface can be classified by homotopy equivalence.

2.2. Uniformization Metric

Let M be a surface embedded in R^3. The total Gaussian curvature of M is solely determined by the topology of the surface, as shown below:

Theorem 1 (Gauss-Bonnet Theorem [41]). *The total Gaussian curvature of a compact surface M is given by*

$$\int_M K dA + \int_{\partial M} k_g ds = 2\pi\chi(M), \tag{1}$$

where K is the Gaussian curvature on interior points, K_g is the geodesic curvature on boundary points, $\chi(M)$ is the Euler characteristic number of M.

Let g be the Riemannian metric of M induced from its Euclidean metric in R^3. Suppose $u : M \to R$ is a scalar function defined on M. Then $\bar{g} = e^{2u}g$ is also a Riemannian metric on M and is conformal to the original one. Any surface admits a Riemannian metric of constant Gaussian curvature, which is conformal to the original metric. Such metric is called the uniformization metric.

Theorem 2 (Uniformization Theorem [29]). *Let $(M, \mathbf{g})$ be a compact 2-dimensional Riemannian manifold with Riemannian metric $\mathbf{g}$ and negative Euler characteristic $\chi < 0$. There exists a Riemannian metric $\bar{\mathbf{g}}$ such that $\bar{\mathbf{g}}$ induces constant -1 Gaussian curvature everywhere of M and is conformal to $\mathbf{g}$.*

According to the Gauss-Bonnet theorem, the sign of the constant Gaussian curvatures is determined by the Euler characteristic of the surface. So surfaces with negative Euler characteristics (i.e., $\chi < 0$) have hyperbolic uniformization metric with -1 Gaussian curvature everywhere.

The geodesics are the locally shortest curves on surfaces. They are defined closely related to metric. The geodesic lengths reflect the global information of the surface. For general surfaces with Euclidean metric, there may be multiple globally shortest and many locally shortest geodesics in each homotopy class. For surfaces with hyperbolic uniformization metric, there exists only one unique globally shortest geodesic and no any other locally shortest geodesics in each homotopy class, which can be directly deduced from the following theorems:

Theorem 3 (Geodesic Uniqueness). *Suppose* $(M, \mathbf{g})$ *is a closed compact surface with metric* $\mathbf{g}$*. If Gaussian curvature is negative everywhere, then each homotopy class has a unique globally shortest geodesic and no other locally shortest geodesics.*

Proof. Given two loops γ_1 and γ_2 on M homotopic to each other, suppose both of them are closed geodesics on M, either globally or locally shortest. If γ_1 and γ_2 contain no points in common, then they bound a topological cylinder C. According to the Gauss-Bonnet theorem, the cylinder satisfies $\int_C KdA + \int_{\partial C} k_g ds = 0$ because the Euler characteristic of a cylinder is zero. From the left side, $k_g = 0$ on both γ_1 and γ_2, so $\int_{\partial C} k_g ds = 0$. Then $\int_C KdA$ has to be zero. Considering that K is negative everywhere, the area of the cylinder is zero, which contradicts the assumption that γ_1 and γ_2 contain no points in common. Therefore γ_1 and γ_2 have at least one intersection point. Suppose they bound a topological disk D. D satisfies $\int_D KdA + \int_{\partial D} k_g ds = 2\pi$ because the Euler characteristic of a disk is one. Since any part of γ_1 or γ_2 is still a geodesic, $k_g = 0$ on the boundary of D, and $\int_{\partial D} k_g ds = 0$. Then $\int_D KdA$ is larger than zero, but this contradicts the given fact that K is negative everywhere. Therefore, γ_1 and γ_2 can't be both homotopy geodesics on M. We conclude that there exists only one closed geodesic given a homotopy type of M and that one is globally shortest. □

Note that the above proof has assumed no self-intersection. If the homotopy class of the given two loops is complicated, they may have self-intersections. The loops are not an embedding, but an immersion on M. We can lift the two loops to the universal covering space of M. In universal covering space, they won't have self-intersections. We can then apply similar argument as the above.

For surfaces with boundaries, proof of geodesic uniqueness can be found in [40].

Corollary 1. *Each homotopy class has a unique globally shortest geodesic and no other locally shortest geodesics for surface* $(\chi < 0)$ *with hyperbolic uniformization metric.*

The proof is straightforward based on the Geodesic Uniqueness theorem.

2.3. Surface Ricci Flow

In order to induce hyperbolic uniformization metric on a surface with $(\chi < 0)$, we will use Ricci flow, which will be described in this section.

Ricci flow on a surface deforms the surface's Riemannian metric according to curvature; suppose the surface M is with area A and Euler characteristic χ, then the time-varying metric $g(t)$ and Gaussian curvature $K(t)$ are related by a heat-like diffusion process,

$$\frac{dg_{ij}(t)}{dt} = -2K(t)g_{ij}(t) + \frac{\chi(M)}{A}.$$

The seminal work on Ricci flow, by Richard Hamilton in 1982, applies to Riemannian manifolds in any dimension [42].

For closed surfaces with $\chi \leq 0$, Hamilton proved:

Theorem 4 (Hamilton 1988). *For a closed surface with $\chi \leq 0$, if the total area of the surface is preserved during the flow, the Ricci flow will converge to a metric such that the induced Gaussian curvature is constant everywhere.*

In discrete case, smooth surface can be approximated by simplicial complex, which is easy to convert to a triangular mesh. Let $M = (V, E, F)$ denote a triangulated surface embedded in $\mathbb{R}^3$, consisting of vertices (V), edges (E), and triangle faces (F). Denote θ_i^{jk} the corner angle attached to $v_i \in V$ in $f_i^{jk} \in F$, and ∂M the boundary of M, discrete Gaussian curvature K_i on v_i is defined as the angle deficit:

$$K_i = \begin{cases} 2\pi - \sum_{f_i^{jk} \in F} \theta_i^{jk}, & v_i \notin \partial M, \\ \pi - \sum_{f_i^{jk} \in F} \theta_i^{jk}, & v_i \in \partial M. \end{cases} \tag{2}$$

A discrete metric on M is a function defined on the set of edges $l : E \to \mathbb{R}^+$ satisfying triangle inequality: $l_{ij} + l_{jk} > l_{ki}$ for each f_{ijk}. We can define a discrete Riemannian metric on M by taking the length of each e_{ij} as its l_{ij}. The discrete Riemannian metric induces a hyperbolic circle packing metric, denoted (M, Γ, Φ). Each v_i associates a hyperbolic circle with radius γ_i. The radius function is defined $\Gamma : V \to \mathbb{R}^+$. The two circles at v_i and v_j of edge e_{ij} intersect with an acute angle ϕ_{ij}, denoted the *weight* of e_{ij}. The weight function is defined $\Phi : E \to [0, \frac{\pi}{2}]$.

The length l_{ij} of e_{ij} can then be computed from the hyperbolic circle packing metric based on the following hyperbolic cosine law:

$$cosh l_{ij} = \cosh \gamma_i \cosh \gamma_j + \sinh \gamma_i \sinh \gamma_j \cos \phi_{ij}. \tag{3}$$

Associate M with an initial hyperbolic circle packing metric (Γ_0, Φ). Let

$$u_i = \log \tanh \frac{\gamma_i}{2} \tag{4}$$

for each v_i, denote t the time, the discrete hyperbolic surface Ricci flow is defined as follows:

$$\frac{du_i(t)}{dt} = -K_i. \tag{5}$$

Chow and Luo [43] have shown that the discrete Ricci flow of Eqn. 5 can be interpreted as the negative gradient flow of a convex energy function with a unique global minimum. They name this the *discrete hyperbolic Ricci energy*, and use it to induce a hyperbolic uniformization metric on the surface.

3. Birkhoff Curve Shortening

In this paper we use Birkhoff curve shortening [30, 44] to find the geodesic homotopic to the original curve. To describe it, we begin with some definitions.

In continuous mathematics on a smooth manifold M, the *injective radius* of a point $p \in M$ is defined as the largest radius for which the exponential map at p is a diffeomorphism. Injective radius can be defined operationally for discrete surfaces as well: choose a tangent plane at p. For each direction v in the plane, trace a geodesic on the surface from p in direction v to a point at distance t, denoted $q_v(t)$. The points at distance t for all directions is a geodesic circle, and the map from this circle to the circle centered at p and of radius t on the tangent plane is called the *exponential map*. As the geodesic circle grows and may touch itself, defining the injective radius of p where the exponential map is no longer 1-to-1 at the touching point. The minimum of the injective radii among all points, denoted as r, is called the injective radius of M. Any two points $p, q \in M$ with $d(p, q) < r$ can be joined by a unique local minimal geodesic.

Let γ^0 be a closed curve in M. We divide γ^0 into n segments with division points $p_1, p_2, ..., p_n$. Such subdivision is fine enough that ensures the distance of nearby division points within distance r. We then replace each arc $\widetilde{p_i p_{i+1}}$ with the geodesic $\overline{p_i p_{i+1}}$ connecting p_i to p_{i+1} and update γ^0 to:

$$\gamma^1 = \overline{p_1 p_2} \bigcup \overline{p_2 p_3} \bigcup ... \bigcup \overline{p_{n-1} p_n}.$$

The length of γ^1 is strictly smaller than the length of γ^0 unless $\gamma^1 = \gamma^0$. Note that the homotopy type of γ^1 won't get changed because each arc is within distance r.

Successive midpoints of the n segments of γ^1 are also within distance r from each other. We then replace the arc connecting them with geodesics. This produces a new loop γ^2. By iterating this process, each new loop is always homotopic to the previous one. We prove that the algorithm converges for surfaces with hyperbolic uniformization metric, and the final loop is the unique homotopy geodesic.

Corollary 2. *For a closed compact surface M with hyperbolic uniformization metric, a loop on M converges to the unique homotopy geodesic with the Birkhoff curve shortening.*

Proof. Denote γ^k the k-th iteration of the Birkhoff curve shortening process for curve γ^0 on M. Denote v_1^k, v_2^k, ... v_n^k the nodes connecting piecewise geodesic curves of γ^k. The distance of v_i^k and v_{i+1}^k is less than the injective radius r of M, that ensures the homotopy class doesn't change during the loop shortening process. The curve shortening process will eventually converge because the length of γ^k decreases and is bounded.

Denote $C = \{\gamma^k | k = 1, 2, ..., \infty\}$ the curve sequence. For a compact surface M, there is a subsequence $C_1 \subset C$, such that $v_1^k \in C_1$ converges; a subsequence $C_2 \subset C$, such that $v_2^k \in C_2$ converges, etc.

Denote v_1 the limit of $v_1^k \in C_1$, v_2 the limit of $v_2^k \in C_2$, etc. Connect each v_i and v_{i+1} by geodesic, and denote γ the final loop.

We show that the intersection angle of the two geodesics connecting v_{i-1} and v_i, and v_i and v_{i+1} at node v_i is zero. If the angle is not zero, we can apply Birkhoff curve shortening process on γ. The length of γ will decrease based on triangle inequality, that contradicts that the length of γ is the inf of all curves in C.

Each segment on γ is a geodesic. Intersection angles of successive geodesic segments are zero, so γ is a geodesic loop. Based on the Geodesic Uniqueness theorem, γ is the only geodesic in the homotopy class. □

In this paper, the parametrization domain for us to compute the geodesics and middle points during the Birkhoff Curve Shortening process is Poincaré disk. We first give a brief introduction of Poincaré disk and refer the reader to [45] for details concerning models of hyperbolic geometry. We will give details of the algorithm later in Section 4.4.

Poincaré Disk. The Poincaré disk is a unit disk on the complex plane with Riemannian metric defined as

$$ds^2 = \frac{4dwd\bar{w}}{(1-\bar{w}w)^2}.$$

In the Poincaré disk, rigid motion is a Möbius transformation,

$$z \to e^{i\theta}\frac{z-z_0}{1-\bar{z}_0 z}, z_0 \in \mathbb{C}, \theta \in [0, 2\pi);$$

the geodesics are circular arcs which are orthogonal to the unit circle; the hyperbolic circle with center $\mathbf{c}$ and radius r, denoted $(\mathbf{c}, r)$, coincides with an Euclidean circle $(\mathbf{C}, R)$ with

$$\mathbf{C} = \frac{2-2\mu^2}{1-\mu^2|\mathbf{c}|^2}\mathbf{c}, \quad R^2 = |\mathbf{C}|^2 - \frac{|\mathbf{c}|^2-\mu^2}{1-\mu^2|\mathbf{c}|^2}, \tag{6}$$

where $\mu = tanh(\frac{r}{2})$.

4. Algorithm

4.1. Overview of the Algorithm

Given a triangular manifold M with $\chi < 0$, we adopt discrete surface Ricci flow method [46] to compute surface hyperbolic uniformization metric in Sec. 4.2. Since it is the most time consuming step and we need only to compute once for all, we store the computed metric - a positive real number - at each edge. In Sec. 4.3, we introduce a combinatorial algorithm to quickly approximate the injective radius r of M. In Sec. 4.4, we give the details of the loop shortening algorithm. For a given closed cycle on M, we first divide it into small subintervals such that each subinterval is less than r. We then repeatedly embed a chart containing each subinterval isometrically to Poincaré disk and compute the middle point of the geodesic connecting the two ending points of the subinterval. After connecting the middle points of neighboring subintervals, we construct a new cycle homotopic to and with length less than the original one. We repeat this process such that each iteration always generates a new loop homotopic to the previous one but with shorter length until the cycle converges to the globally shortest geodesic in its homotopy type. Figure 3 illustrates the algorithm.

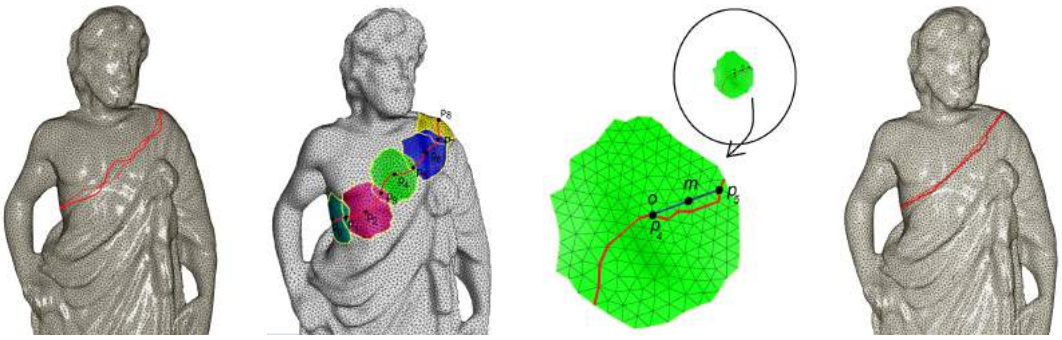

Figure 3: Algorithm illustration: (a) the input loop γ is marked with red on a triangular manifold M; (b) loop γ is divided by points $p_0, p_1, ..., p_{n-1}$ into n segments such that each segment is shorter than the injective radius r of M. One chart will cover one segment with color marked. Here we only show part of those charts which cover even number segments for illustration. (c) One chart is isometrically parameterized into the Poincaré disk with one of the two division points (it is p_4 in this example) in the center of the disk. So the geodesic path between p_4 and p_5 in the Poincaré disk coincides with an Euclidean straight line, marked with blue. m is their middle point. (d) By connecting the n midpoints of the segments with geodesic paths, a new closed loop $\bar{\gamma}$ is produced, shorter than and homotopic to γ.

4.2. Pre-computing the Hyperbolic Uniformization Metric

For a given triangle mesh M with vertex set V, edge set E, face set F, the algorithm to compute surface hyperbolic uniformization metric can be summarized as the following:

1. We first initiate a hyperbolic circle packing metric from the discrete Riemannian metric of M induced by edge length. For each vertex v_i, denote m the number of its adjacent faces, and l_{ij}, l_{jk}, l_{ki} the edge lengths of e_{ij}, e_{jk}, and e_{ki} respectively, compute its initial circle radius γ_i by averaging its adjacent face radius:

$$\gamma_i = \frac{1}{m} \sum_{f_{ijk} \in F} \frac{l_{ki} + l_{ij} - l_{jk}}{2};$$

   for each edge e_{ij}, compute its edge weight ϕ_{ij} from γ_i, γ_j according to Eqn. 3.

2. For each vertex v_i, compute its current discrete Gaussian curvature K_i according to Eqn. 2, where the corner angle θ_i^{jk} in each adjacent face f_{ijk} is computed based on the hyperbolic cosine law:

$$\cosh l_{ij} = \cosh \gamma_i \cosh \gamma_j + \sinh \gamma_i \sinh \gamma_j \cos \theta_i^{jk}. \tag{7}$$

3. For each vertex v_i, set the step length ϵ no greater than 0.1, update its u_i defined in Eqn. 4 as

$$u_i = u_i + \epsilon(-K_i).$$

   Update its radius γ_i according to Eqn. 4 correspondingly.
4. For each edge l_{ij}, update its edge length with current vertices radii γ_i and γ_j and the edge weight ϕ_{ij} according to Eqn. 7.
5. Repeat the steps from 2 through 4, until the maximal curvature error falls below a user-specified error tolerance threshold δ.

$$\max |\bar{K}_i - K_i| < \delta.$$

   In our experiments, we set it to $1e-5$, which is good enough without folding or overlapping found.

As mentioned in Section 2, discrete Ricci flow is the negative gradient flow of the discrete Ricci energy with a unique global minimum which induces the uniformization metric. Instead of the above gradient descent method, we can apply Newton's method to compute surface hyperbolic uniformization metric. The key to Newton's method is to compute the Hessian matrix, which can be computed explicitly. Please refer [46] for the closed form.

4.3. Estimation of Chart Size

Birkhoff curve shortening process requires the maximal segment length no longer than the injective radius of the manifold. While for a given loop, the convergence speed with the curve shortening process is related to the number of segments. In general, the more segments, the more time is needed for each iteration, unless they are computed in a parallel way. Also, the smaller each segment, the slower the overall convergence speed is. Considering this dilemma, we compute an approximation of the injective radius and set as the maximal length of each segment.

The following algorithm computes an approximation of the injective radius of a triangular surface. The basic idea is to grow a disk as big as possible

with the center at a vertex of the surface before the boundary of the disk meets from different directions. The difficulty is to distinguish whether the disk meets from one direction due to the discrete structure of the surface or different directions. We associate each edge with two directions. e_{ij} indicates one direction from v_i to v_j and e_{ji} with the reverse direction. Each face f_{ijk} has a CCW orientation indicated by its vertex sequence.

1. For each vertex v_i, initialize an empty boundary list L_i associated with v_i.
2. Randomly mark one face f_{ijk} which contains vertex v_i, and update the list L_i to $\{e_{ij}, e_{jk}, e_{ki}\}$. Note that the sequence and the directions of the edges are consistent with the CCW orientation of f_{ijk}.
3. Mark the neighboring faces of f_{ijk} if they have not been marked by v_i. For example, f_{jil} has not been marked by v_i. Then mark f_{jil} and update the list L_i by replacing e_{ij} with e_{il}, e_{lj}. The boundary list L_i is $\{e_{il}, e_{lj}, e_{jk}, e_{ki}\}$.
4. Continue to grow the disk centered at v_i. After each iteration of marking those non-marked faces along the current boundary of disk and correspondingly updating the boundary list, the list L_i needs be checked to remove those edges which appear successive but with opposite directions, like e_{ij}, e_{ji}. The list will keep checking until no more edges can be removed. Note that the first edge in the list is considered successive with the last one in L_i.
5. The disk will stop growing as soon as there is one edge that appears twice in the list can't be removed.
6. Each vertex will compute a disk with a radius following the above method. Then we choose the smallest radius r among the computed radii, and set as a threshold that no segment of a divided loop can be longer than r.

The above algorithm is efficient but provides only an approximation based on the combinatorial structure of the surface, which depends on the triangulation quality of the surface and prefers a uniform one. If the triangulation is extremely irregular, the disk can grow based on geodesic offsets with the price of high computation cost. The algorithm proposed by [47] can be adapted by replacing the Euclidean metric with the hyperbolic uniformization metric.

4.4. Loop Shortening

We first divide a given loop γ on M into n segments with the length of each segment less than the computed r, as one example given in Figure 3 (a). For a segment with two ending vertices p_i and p_{i+1}, we locally construct a chart, denoted as C, which fully covers the segment as shown in Figure 3 (b) and isometrically embed C to the Poincaré disk based on the pre-computed hyperbolic uniformization metric as shown in Figure 3 (c). Denote the embedding function as $uv : V \to \mathbb{H}^2$. The following algorithm gives the details.

1. Start from vertex p_i (v_i), we randomly pick one of its neighboring triangles f_{ijk} to embed to the Poincaré disk, with

$$uv(v_i) = (0, 0), uv(v_j) = (\tanh \frac{l_{ij}}{2}, 0),$$

$$uv(v_k) = (\tanh \frac{l_{ik}}{2} \cos \theta_0^{jk}, \tanh \frac{l_{ik}}{2} \sin \theta_0^{jk}).$$

   Here, l_{ij} is the hyperbolic uniformization metric of edge e_{ij}. Then we put all the neighboring triangles of f_{ijk} to a queue Q.
2. Pop out the first triangle f_{ijl} from Q. Suppose except v_l, v_i and v_j have been embedded to the Poincaré disk with $uv(v_i)$ and $uv(v_j)$ respectively. The coordinates of v_l can be computed as one of the intersection points of the two hyperbolic circles

$$(uv(v_i), l_{il}) \cap (uv(v_j), l_{jl}),$$

   with centers $uv(v_i)$ and $uv(v_j)$ and radii l_{il} and l_{jl} respectively, and satisfying

$$(uv(v_j) - uv(v_i)) \times (uv(v_l) - uv(v_i)) > 0.$$

   Since hyperbolic circles in the Poincaré disk coincide with Euclidean circles, computing the intersection points between two hyperbolic circles boils down to finding intersections between two Euclidean circles (see Eqn. 6). Then we put all the neighboring triangles of f_{ijl} to Q.
3. We keep growing and embedding the chart with such a breadth first search, until all the neighboring triangles of vertex p_{i+1} have been embedded to the Poincaré disk.

Since p_i is embedded in the center of the Poincaré disk, the hyperbolic geodesic connecting p_i and p_{i+1} coincides with the Euclidean straight line connecting p_i and p_{i+1}, as illustrated in Figure 3 (c). We can explicitly compute the geodesic by splitting crossing edges embedded in the Poincaré disk with the straight line. Then we project it back to the surface. By replacing each segment with its geodesic on surface, the new loop $\bar{\gamma}$ is shorter than the original γ.

For further shortening, the middle point of a segment with ending vertices p_i and p_{i+1} can be computed directly from the following formula on the embedded chart containing the segment:

$$m = \frac{1+\mu^2}{2} uv(p_{i+1}),$$

where

$$\mu = tanh(\frac{r}{2}), r = \frac{1}{2} log \frac{1+|uv(p_{i+1})|}{1-|uv(p_{i+1})|}.$$

The geodesic connecting two successive middle points can be constructed in the similar way of computing the geodesic connecting two successive subinterval points. By joining every two successive middle points with a geodesic, this produce a new loop $\bar{\bar{\gamma}}$, shorter than $\bar{\gamma}$, as illustrated in Figure 3 (d). For each iteration, we record the current length of the loop. We stop the iteration if the difference of the lengths of the loop between two successive iterations is less than a threshold. We set the threshold to $1e-3$.

Unless we want to visualize the deformation process, we don't need to explicitly compute and project each geodesic segment back to the original surface. For each iteration, we need only a list of middle points in sequence. Since the parameterized charts on Poincaré disk differ only by Möbius transformations for overlapping parts, and cross ratio is invariant. To record the position of the middle point on surface independent of the local chart, we need to store the cross ratio of the point instead of its barycentric coordinates. For one middle point P, located inside face f_{ijk}, its cross ratio can be computed as

$$(uv(v_i), uv(v_j); uv(v_k), uv(P)) = \frac{(uv(v_i) - uv(v_k))(uv(v_j) - uv(P))}{(uv(v_j) - uv(v_k))(uv(v_i) - uv(P))}.$$

If the input loop is quite long, when the loop has been shrunk much such that the distances between neighboring subdivision points are much less than

the approximate injective radius, we need to merge those neighboring subdivision points to reduce the number of segments to improve the convergence speed, especially for loops which are homotopic to zero.

Table 1: Computing Time. (G is the genus number. F is the face number.)

Model	G	F	Metric Time	Loop	Iterations	Converge Time
Greek	4	25k	130 Sec.	$\gamma 1$	180	20 Sec.
				$\gamma 2$	250	22 Sec.
				$\gamma 3$	150	15 Sec.
				$\gamma 4$	280	24 Sec.

5. Performance Evaluation and Discussions

We implement the algorithms using C++ on a Windows platform and conduct all the experiments on a laptop with 2.5 GHz dual CPU and 4.0 GB RAM. All testing models are triangle surfaces. We apply Newton's method to compute their hyperbolic uniformization metric. Table 1 summarizes the computing time of the uniformization metric and the loop shortening on model shown in Figure 6. Although computing the hyperbolic uniformization metric is time consuming, the efficiency of the whole algorithm won't be jeopardized by this step, because we can pre-compute the hyperbolic uniformization metric and store with edges once for all for mesh models. Figure 4 gives the convergence speed of the length of the loops on model shown in Figure 6.

We test our algorithms on models with different triangulation qualities. The Birkhoff curve shortening process itself is not affected by irregular triangulations, as shown by examples in Figure 5. Loops with the same homotopy type shrink to the unique homotopy geodesic of a mesh model with different triangulations. Irregular triangulations do affect the numerical stability and the convergence speed to compute surface hyperbolic uniformization metric, which is the biggest constraint of our algorithms. For extremely skinny triangles, we check and perform a local edge flip.

As detailed in Sec. 4.3, we set the injective radius of a manifold as the maximal length of each segment, but it is not necessary. A geodesic between

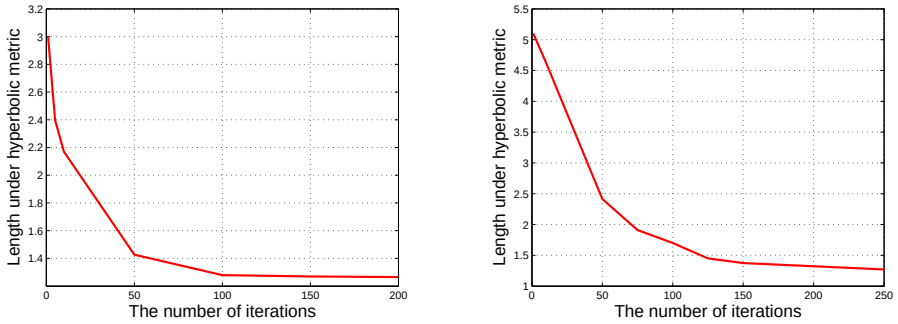

(a)Loop γ_1 (b) Loop γ_2

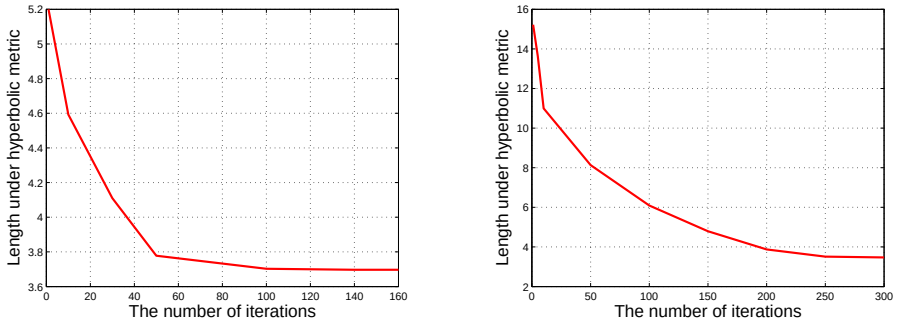

(c) Loop γ_3 (d) Loop γ_4

Figure 4: The convergence of the lengths of the loops shown in Figure 6 after a number of iterations.

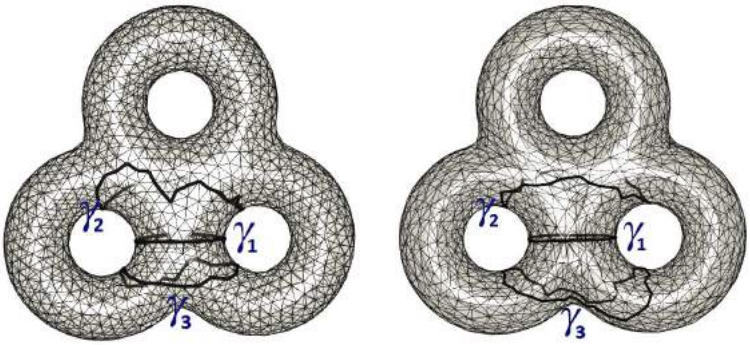

(a) (b)

Figure 5: Loops shrink to the unique geodesic γ_1 of the same homotopy type with the same mesh model approximated by different triangulations.

(a)Loop γ_1 (b) 6 iterations (c) 9 iterations (d) 50 iterations

(f) Loop γ_2 (g) 10 iterations (h) 50 iterations (i) 100 iterations

(k) Loop γ_3 (l) 10 iterations (m) 50 iterations (n) 100 iterations

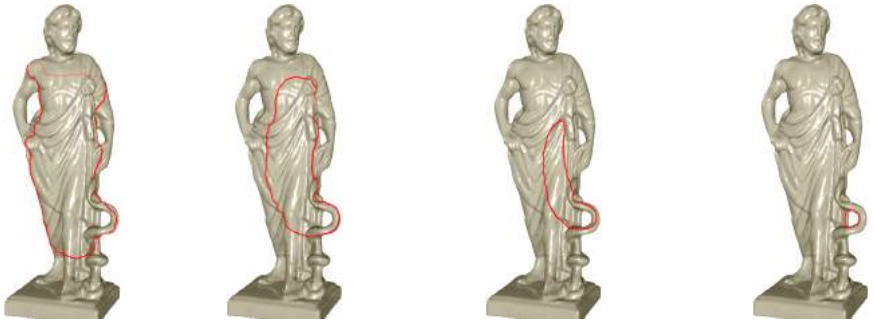

(p) Loop γ_4 (q) 30 iterations (r) 100 iterations (s) 200 iterations

Figure 6: Visualization of loop shortening on Greek model.

points p and q is *local* and can be computed exactly if it is within the injective radius of both p and q, and a replacement of an arc connecting p and q with the geodesic won't change the homotopy type. We can store the injective radius of each vertex and dynamically determine the maximum length of each segment based on the values stored at vertices along the loop. The convergence speed of loop shortening can improve slightly compared with a fixed maximum segment length, although experimental results given in this paper are all based on injective radius of a manifold.

Note that the unique geodesic homotopic to the given cycle computed in this paper is based on surface hyperbolic uniformization metric instead of surface Euclidean metric. It is well known that these unique closed geodesics form a so called geodesic spectrum of the surface with $\chi < 0$ and represent the surface conformal structure which is invariant under conformal deformations. Surface conformal structure is much coarser than surface geometric structure, so theoretically the computed unique geodesic under one homotopy type should be stable under small geometry perturbations. It is unknown to us how the geodesic under surface hyperbolic uniformization metric relates with the globally shortest geodesics under surface Euclidean metric with the same homotopy type. In our experimental results, as one example given by Figure 7 with a set of geodesics (seven loops) computed on two models respectively, some coincide perfectly, but some differ a lot.

6. Applications

6.1. Extremal Quasiconformal Mapping

Given a Riemann surface M, the Teichmüller shape space T_M is a complex manifold whose points represent all complex structures of Riemann surfaces with the same topological structure of M. Teichmüller shape space provides a theoretically sound foundation for surface classification, where surfaces are classified based on conformal equivalence relation. Specifically, in this space, each point represents a class of conformal equivalent surfaces where there exist conformal deformations (i.e., angle preserved deformations) among them. A curve connecting any two points represents a quasiconformal deformation (i.e., bounded angle distorted deformations) between two classes of conformally inequivalent compact Riemann surfaces. A geodesic between the two points represents an extremal quasiconformal deformation, the one minimizing the angular distortion among all possible diffeomorphisms between the two classes of surfaces. Such extremal quasiconformal mapping is unique

and always exists [48, 49, 50]. extremal quasiconformal mapping provides not only the measurement of the geometric difference between two topologically equivalent surfaces for shape space, but also an automatic mapping between two shapes with the least angle distortion which is highly preferred by many graphics and modeling related applications.

There is no computational algorithm so far to directly compute extremal quasiconformal mapping. However, given a topologically nontrivial surface, we can sort all its unique closed geodesics - shortest homotopic cycles - according to their lengths under the measurement of surface hyperbolic uniformization metric. They form a geodesic spectrum and represent the signature of the surface conformal structure. If the conformal structures of two given surfaces are close, their geodesic spectra are also close. More explicitly, not only the lengths of the geodesics, but also their distribution on the surface and the skeleton formed by them are also similar. Therefore, the closed geodesics under the hyperbolic uniformization metric are the major feature curves of the surface. They capture the conformal structure of the shapes. We can use geodesic spectrum to guide us to approximate the extremal quasiconformal mapping between surfaces with similar shapes and the same non-trivial topology to achieve less angle distortions.

Since there are infinite number of homotopy types in a general non-trivial topology surface, we only use a partial geodesic spectrum, and allow the user to choose. Then for surfaces with the same topology and similar geometric shapes, they may share similar geodesic spectrums, which segment the surfaces into corresponding patches. The global mapping is reduced to a set of mappings between pairs of corresponding surface patches. The mapping between pair of surface patches can be induced from a conformal map between parameterized patches in 2D plane [46]. Figure 7 gives one example.

Texture transfer is the best way to intuitively visualize the globally least angle distortion property of the computed map between surfaces. As shown in Figure 8, we first compute a conformal map of the amphora model to plane [46], and then project a planar blackboard texture back to the model based on the inverse of the conformal map, which can be visualized by the preservation of the right angles. We transfer the texture from the amphora model to the vase model based on the computed extremal quasiconformal mapping between the two models. The texture transfer from the top teapot model to the bottom teapot model is in a similar way. Surface morphing is another way to visualize the mapping result. Figure 9 shows the surface mapping results by conducting linear interpolation between source and target surfaces

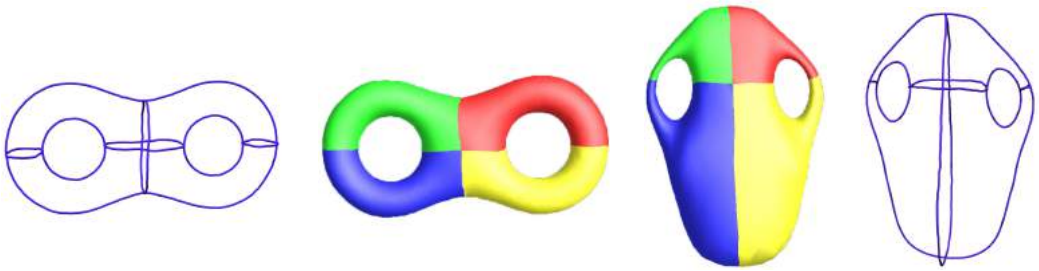

(a) (b) (c) (d)

Figure 7: (a)(d) Geodesic spectra of the eight model and the vase model; (b)(c) surfaces are segmented to a set of patches, same color for corresponding pair of patches.

to generate the morphing process. For the last two morphing examples, the original models are genus zero surfaces. By topological surgery, adding cuts on the hands and feet for the girl models, cuts on the tips of fingers for the hand models, these models are converted to closed high genus surfaces after double covering (gluing two copies of a same open surface along their boundaries).

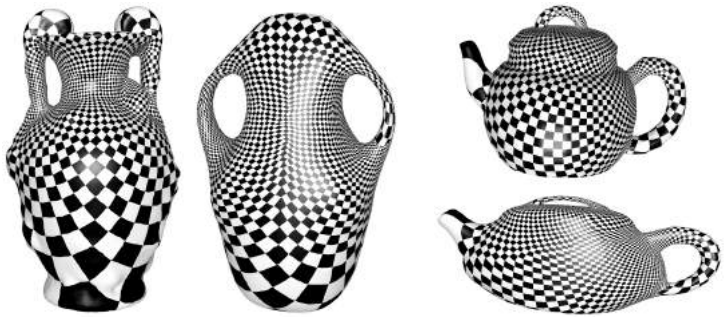

(a) (b)

Figure 8: Texture transfer based on surface mapping: (a) an amphora model transfers its checkboard texture to a vase model based on the mapping between them; (c) the top teapot model transfers its checkboard texture to the bottom teapot model based on the mapping between them.

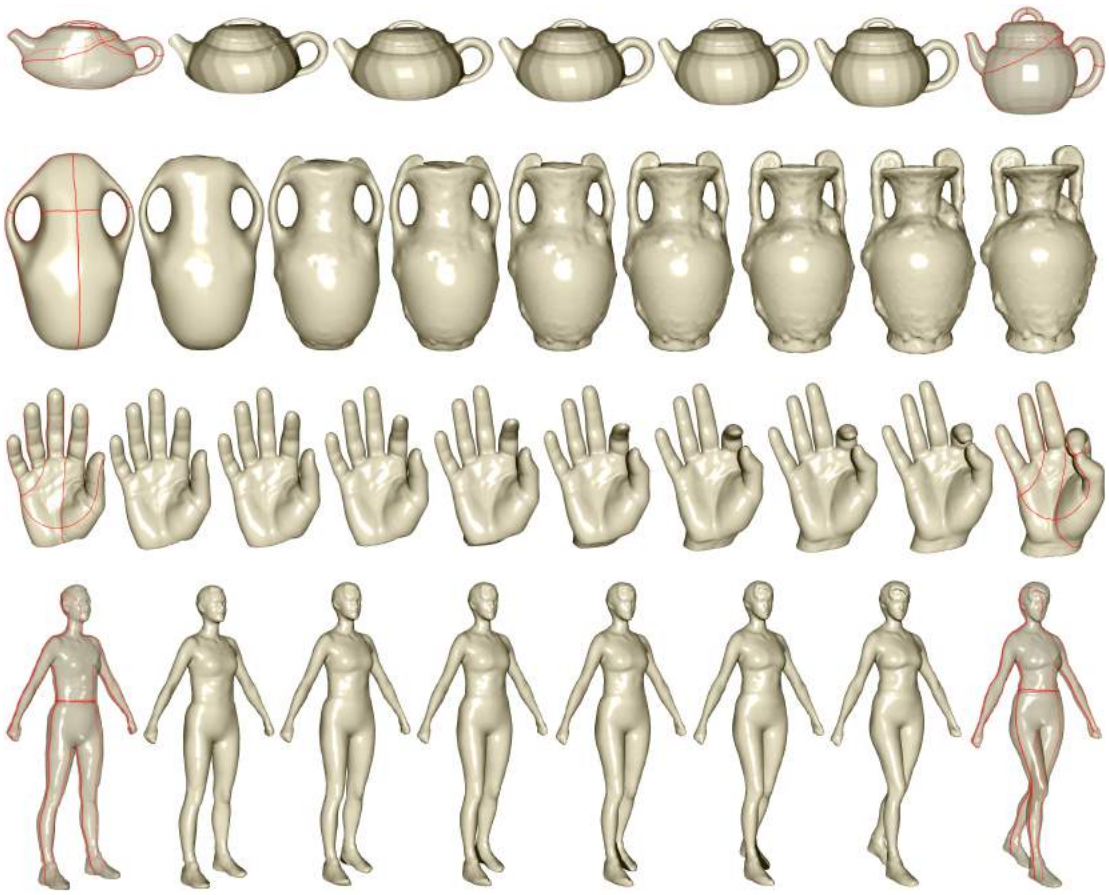

Figure 9: Geodesic spectrum based surface mapping visualized by surface morphing. Red loops on source and target surfaces are computed geodesic spectrum.

6.2. Homotopy Detection

A basic topological problem is to determine whether two paths p_1 and p_2 that start and end at the same points or two cycles l_1 and l_2 are homotopic to each other or not. We can apply our algorithms for homotopy detection. If two cycles γ_i and γ_j are homotopic to each other, they can shrink to the unique homotopy geodesic γ under the given algorithms; if two paths l_1 and l_2 are homotopic to each other, the closed loop $l_1 l_2^{-1}$ which concatenates l_1 with the reverse of l_2, can shrink to a point on the surface. One example is given on the Pegasus model in Figure 10. After 150 iterations, five different loops $\gamma_1, \gamma_2, \gamma_3, \gamma_4, \gamma_5$ on the surface as shown in Figure 10(a) shrink to three geodesics and one point as shown in Figure 10(c), which indicates that γ_2 and γ_5 are homotopic to each other, and γ_1 is topologically trivial.

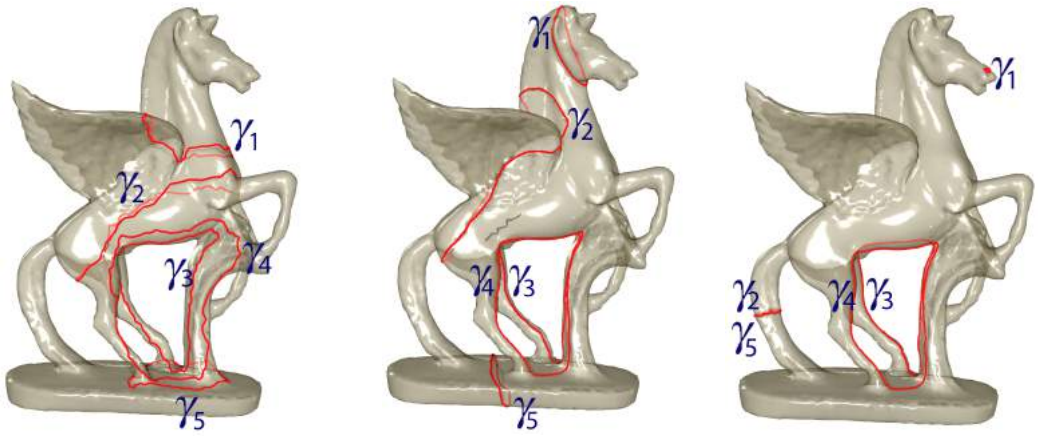

(a) Loops on Pegasus model (b) After 10 iterations (c) After 100 iterations

Figure 10: Homotopy Detection: (a) five different loops $\gamma_1, \gamma_2, \gamma_3, \gamma_4, \gamma_5$ on Pegasus model; (b) after 10 iterations; (c) after 100 iterations.

7. Conclusion And Future Work

In this paper, we adopt a simple local shortening algorithm, Birkhoff Curve Shortening, to compute the shortest cycle homotopic to a given cycle on triangular surfaces with $\chi < 0$ based on surface hyperbolic uniformization metric. We then apply our algorithm to approximate the extremal quasi-conformal mapping between two topologically equivalent surfaces. Such a

mapping exists and a computational algorithm would benefit many computer graphics and geometric modeling related applications. We show texture transfer and morphing as direct applications of the constructed extremal quasiconformal mapping between surfaces. We also apply our algorithm to a classical computational topology problem, homotopy detection of paths and cycles on surfaces.

In the future, we plan to utilize the parallel capability of the programmable graphics processing unit (GPU) to accelerate the algorithm, such that for each iteration, the computation of the middle points of segments can be conducted simultaneously. We also plan to apply and compare more local loop shortening algorithms on hyperbolic space.

References

[1] H. Schipper, Determining contractibility of curves, in: Proceedings of the eighth annual symposium on Computational geometry, 1992, pp. 358–367.

[2] T. K. Dey, H. Schipper, A new technique to compute polygonal schema for 2-manifolds with application to null-homotopy detection, in: Discrete and Computational Geometry, Vol. 14, 1995.

[3] T. K. Dey, S. Guha, Transforming curves on surfaces, J. Comput. Syst. Sci. 58 (1999) 297–325.

[4] E. Colin de Verdière, F. Lazarus, Optimal system of loops on an orientable surface, in: Proceedings of the 43rd Symposium on Foundations of Computer Science, 2002, pp. 627–636.

[5] E. Colin de Verdière, F. Lazarus, Optimal pants decompositions and shortest homotopic cycles on an orientable surface, Journal of the ACM 54 (4) (2007) 1–1.

[6] J. Erickson, S. Har-Peled, Optimally cutting a surface into a disk, in: Proceedings of the eighteenth annual symposium on Computational geometry, 2002, pp. 244–253.

[7] E. Colin de Verdière, Shortest cut graph of a surface with prescribed vertex set, in: Proceedings of the 18th annual European conference on Algorithms: Part II, 2010, pp. 100–111.

[8] T. K. Dey, K. Li, J. Sun, D. Cohen-Steiner, Computing geometry-aware handle and tunnel loops in 3d models, in: ACM SIGGRAPH, 2008, pp. 1–9.

[9] J. Erickson, K. Whittlesey, Greedy optimal homotopy and homology generators, in: Proceedings of the sixteenth annual ACM-SIAM symposium on Discrete algorithms, 2005, pp. 1038–1046.

[10] M. Kutz, Computing shortest non-trivial cycles on orientable surfaces of bounded genus in almost linear time, in: SCG '06: Proceedings of the twenty-second annual symposium on Computational geometry, 2006, pp. 430–438.

[11] S. Cabello, E. Colin de Verdière, F. Lazarus, Finding shortest non-trivial cycles in directed graphs on surfaces, in: Proceedings of the 2010 annual symposium on Computational geometry, 2010, pp. 156–165.

[12] J. Erickson, P. Worah, Computing the shortest essential cycle, Tech. rep. (2010).

[13] S. Bischoff, L. Kobbelt, Structure preserving CAD model repair, Comput. Graphics Forum 24 (2005) 527–536.

[14] Q.-Y. Zhou, T. Ju, S.-M. Hu, Topology repair of solid models using skeletons, IEEE Transactions on Visualization and Computer Graphics 13 (4) (2007) 675–685.

[15] P. Alliez, E. Colin de Verdière, O. Devillers, M. Isenburg, Centroidal Voronoi diagrams for isotropic surface remeshing, Graphical Models 67 (3) (2005) 204–231.

[16] X. Li, X. Gu, H. Qin, Surface mapping using consistent pants decomposition, IEEE Transactions on Visualization and Computer Graphics 15 (4) (2009) 558–571.

[17] S. Biasotti, D. Giorgi, M. Spagnuolo, B. Falcidieno, Reeb graphs for shape analysis and applications, Theoretical Computer Science 392 (2008) 5–22.

[18] S.-W. Cheng, T. K. Dey, J. A. Levine, A practical Delaunay meshing algorithm for a large class of domains, in: Proceedings of the 16th International Meshing Roundtable, 2007, pp. 477–494.

[19] M. A. Grayson, Shortening embedded curves, Annals of Mathematics 129 (1989) 71–111.

[20] M. Gage, Curve shortening on surfaces, Ann. Scientifiques de L'Ecole Normale Supérieure 23 (2) (1990) 229–256.

[21] Y. Lee, S. Lee, Geometric snakes for triangular meshes, Computer Graphics Forum at Eurographics 21 (3) (2002) 229–238.

[22] L. Ma, D. Chen, Curve shortening flow in a riemannian manifold, in: arXiv:math.DG/0312463v1, 2003.

[23] K. Mikula, D. Sevcovic, Evolution of curves on surface driven by the geodesic curvature and external force, Applicable Analysis 85 (2006) 345–362.

[24] C. Wu, X. Tai, A level set formulation of geodesic curvature flow on simplicial surfaces, IEEE Transactions on Visualization and Computer Graphics 16 (4) (2010) 647–662.

[25] J. Hersberger, J. Snoeyink, Around and around: computing the shortest loop, in: The third Canadian Conference on Computational Geometry, 1991, pp. 157–161.

[26] J. Hersberger, J. Snoeyink, Computing minimum length paths of a given homotopy class, Comput. Geom. Theory Appl. 4 (2) (1994) 63–97.

[27] X. Yin, M. Jin, X. Gu, Computing shortest cycles using universal covering space, Vis. Comput. 23 (12) (2007) 999–1004.

[28] E. Colin de Verdière, J. Erickson, Tightening non-simple paths and cycles on surfaces, in: Proceedings of the seventeenth annual ACM-SIAM symposium on Discrete algorithm, 2006, pp. 192–201.

[29] A. F. Beardon, A Primer on Riemann Surfaces, Cambridge University Press, 1984.

[30] G. D. Birkhoff, Dynamical systems with two degrees of freedom, Trans. Amer. Math. Soc. 18 (1917) 199–300.

[31] J. Hass, P. Scott, Shortening curves on surfaces, Topology 33 (1) (1994) 25–43.

[32] J. S. Mitchell, Geometric shortest paths and network optimization, in: Handbook of Computational Geometry, Elsevier Science Publishers B.V. North-Holland, 1998, pp. 633–701.

[33] W. Zeng, M. Jin, F. Luo, X. Gu, Canonical homotopy class representative using hyperbolic structure, in: IEEE International Conference on Shape Modeling and Applicat, 2009.

[34] X. Yin, Y. Li, W. Han, F. Luo, X. D. Gu, S.-T. Yau, Computing shortest words via shortest loops on hyperbolic surfaces, Computer Aided Design 43 (2011) 1449–1456.

[35] E. W. Chambers, E. Colin de Verdière, J. Erickson, F. Lazarus, K. Whittlesey, Splitting (complicated) surfaces is hard, Comput. Geom. Theory Appl. 41 (2008) 94–110.

[36] C. Chen, D. Freedman, Quantifying homology classes, in: Proc. 25th Ann. Symp. Theoretical Aspects Comput. Sci., 2008, pp. 169–180.

[37] C. Chen, D. Freedman, Hardness results for homology localization, in: Proceedings of the Twenty-First Annual ACM-SIAM Symposium on Discrete Algorithms, 2010, pp. 1594–1604.

[38] J. Erickson, A. Nayyeri, Minimum cuts and shortest non-separating cycles via homology covers, in: Symposium on Discrete Algorithms, 2011.

[39] J. R. Munkres, Elements of Algebraic Topology, Addison Wesley Co., 1984.

[40] P. Buser, Geometry and Spectra of Compact Riemann Surfaces (Progress in Mathematics), Birkhauser, 1992.

[41] A. Pressley, Elementary Differential Geometry, Springer, 2010.

[42] R. S. Hamilton, Three manifolds with positive Ricci curvature, Journal of Differential Geometry. 17 (1982) 255–306.

[43] B. Chow, F. Luo, Combinatorial Ricci flows on surfaces, Journal Differential Geometry 63 (1) (2003) 97–129.

[44] J. E. Borzellino, B. G. Lorica, The closed geodesic problem for compact Riemannian 2-orbifolds, Pacific J. Math. 175 (1) (1996) 39–46.

[45] J. W. Anderson, Hyperbolic Geometry, Springer, 1999.

[46] M. Jin, J. Kim, F. Luo, X. Gu, Discrete surface Ricci flow, IEEE Transactions on Visualization and Computer Graphics 14 (5) (2008) 1030–1043.

[47] S.-Q. Xin, G.-J. Wang, Applying the improved chen and han's algorithm to different versions of shortest path problems on a polyhedral surface, Comput. Aided Des. 42 (2010) 942–951.

[48] O. Teichmüller, Extremale quasikonforme abbildungen und quadratische differentiate, Abh. Preuss. Akad. Wis. Math.-Nat. Kl. 22.

[49] O. Teichmüller, Bestimmung der extremalen quasikonformen abbildung bei geschlossenen orientierten Riemannschen flächen, Abh. Preuss. Akad. Wis. Math.-Mat. Kl. 4 (1943) 1–41.

[50] L. V. Ahlfors, Lectures on quasiconformal maps, Wadsworth Publishing Company, 2006.